Inorganic Chemistry
Article

Inorg. Chem. **2009,** *48,* 4817–4827 **4817**
DOI:10.1021/ic802385c

(Ni_2), (Ni_3), and $(Ni_2 + Ni_3)$: A Unique Example of Isolated and Cocrystallized Ni_2 and Ni_3 Complexes

Pampa Mukherjee,[†] Michael G. B. Drew,[‡] Carlos J. Gómez-García,*[,§] and Ashutosh Ghosh*[,†]

[†]*Department of Chemistry, University College of Science, University of Calcutta, 92, APC Road, Kolkata-700 009, India,* [‡]*School of Chemistry, The University of Reading, P. O. Box 224, Whiteknights, Reading RG 66AD, United Kingdom, and* [§]*Instituto de Ciencia Molecular (ICMol), Parque Científico, Universidad de Valencia, 46980 Paterna, Valencia, Spain*

Received December 15, 2008

Structural and magnetic characterization of compound $\{[Ni_2(L)_2(OAc)_2][Ni_3(L)_2(OAc)_4]\}\cdot 2CH_3CN$ (**3**) (HL = the tridentate Schiff base ligand, 2-[(3-methylamino-propylimino)-methyl]-phenol) shows that it is a rare example of a crystal incorporating a dinuclear Ni(II) compound, $[Ni_2(L)_2(OAc)_2]$, and a trinuclear one, $[Ni_3(L)_2(OAc)_4]$. Even more unusual is the fact that both Ni (II) complexes, $[Ni_2(L)_2(OAc)_2]$ (**1**) and $[Ni_3(L)_2(OAc)_4(H_2O)_2]\cdot CH_2Cl_2\cdot 2CH_3OH$ (**2**), have also been isolated and structurally and magnetically characterized. The structural analysis reveals that the dimeric complexes $[Ni_2(L)_2(OAc)_2]$ in cocrystal **3** and in compound **1** are almost identical-in both complexes, the Ni(II) ions possess a distorted octahedral geometry formed by the chelating tridentate ligand (L), a chelating acetate ion, and a bridging phenoxo group with very similar bond angles and distances. On the other hand, compound **2** and the trinuclear complex in the cocrystal **3** show a similar linear centrosymmetric structure with the tridentate ligand coordinated to the terminal Ni(II) and linked to the central Ni(II) by phenoxo and carboxylate bridges. The only difference is that a water molecule found in **2** is not present in the trinuclear unit of complex **3**; instead, the coordination sphere is completed by an additional bridging oxygen atom from an acetate ligand. Variable-temperature (2−300 K) magnetic susceptibility measurements show that the dinuclear unit is antiferromagnetically coupled in both compounds ($2J = -36.18$ and -29.5 cm^{-1} in **1** and **3**, respectively), whereas the trinuclear unit shows a very weak ferromagnetic coupling in compound **3** ($2J = 0.23$ cm^{-1}) and a weak antiferromagnetic coupling in **2** ($2J = -8.7(2)$ cm^{-1}) due to the minor changes in the coordination sphere.

Introduction

The rational design of solid-state structures is the essence of crystal engineering.[1] Among the different types of solid compounds, multicomponent crystals, known as cocrystals,[2] may be considered as a special class. There is currently intense interest in the design, synthesis, and properties of such molecular cocrystals.[3] Cocrystallization of two different molecules is a possible way of intentionally influencing the position of molecules in a crystal lattice and allows for the investigation of newly generated macroscopic properties. Indeed, cocrystallization studies offer rich opportunities for studying the hierarchy of intermolecular interactions within a crystalline solid. Cocrystals that comprise of two or more molecules (cocrystal formers)[4] that are solids under ambient conditions represent a well-established[5] class of compound. However, they remain rare and thus relatively unexplored; a Cambridge Structural Database (CSD)[6] survey reveals that they represent less than 0.5% of published crystal structures. The three important requirements for cocrystallization

*To whom correspondence should be addressed. E-mail: carlos.gomez@uv.es (C.J.G.-G.); ghosh_59@yahoo.com (A.G.).

(1) (a) Desiraju, G. R. *Crystal Engineering. The Design of Organic Solids*; Elsevier: Amsterdam, 1989. (b) Desiraju, G. R. *Angew. Chem.* **1995**, *107*, 2541. (c) Desiraju, G. R. In *Comprehensive Supramolecular Chemistry*; MacNicol, D. D., Toda, F., Bishop, R., Eds.; Pergamon: Oxford, 1996; Vol. 6, p 1.

(2) (a) Koshima, H.; Nagano, M.; Asahi, T. *J. Am. Chem. Soc.* **2005**, *127*, 2455. (b) Childs, S. L.; Chyall, L. J.; Dunlap, J. T.; Smolenskaya, V. N.; Stahly, B. C.; Stahly, G. P. *J. Am. Chem. Soc.* **2004**, *126*, 13335. (c) Remenar, J. F.; Morissette, S. L.; Peterson, M. L.; Moulton, B.; MacPhee, J. M.; Guzman, H. R.; Almarsson, O. *J. Am. Chem. Soc.* **2003**, *125*, 8456. (d) Zhang, X.-L.; Chen, X.-M. *Cryst. Growth Des.* **2005**, *5*, 617. (e) Keyes, T. E.; Forster, R. J.; Bond, A. M.; Miao, W. *J. Am. Chem. Soc.* **2001**, *123*, 2877. (f) Koshima, H.; Miyamoto, H.; Yagi, I.; Uosaki, K. *Cryst. Growth Des.* **2004**, *4*, 807. (g) Ohba, S.; Hosomi, H.; Ito, Y. *J. Am. Chem. Soc.* **2001**, *123*, 6349. (h) Loehlin, J. H.; Etter, M. C.; Gendreau, C.; Cervasio, E. E. *Chem. Mater.* **1994**, *6*, 1218. (i) Bhogala, B. R.; Nangia, A. *Cryst. Growth Des.* **2003**, *3*, 547. (j) Nayak, M.; Hazra, S.; Lemoine, P.; Koner, R.; Lucas, C. R.; Mohanta, S. *Polyhedron* **2008**, *27*, 1201. (k) Nayak, M.; Koner, R.; Lin, H.-H.; Flörke, U.; Wei, H.-H.; Mohanta, S. *Inorg. Chem.* **2006**, *45*, 10764. (l) Lee, H. M.; Olmstead, M. M.; Gross, G. G.; Balch, A. L. *Cryst. Growth Des.* **2003**, *3*, 691. (m) Olmstead, M. M.; Wei, P.; Ginwalla, A. S.; Balch, A. L. *Inorg. Chem.* **2000**, *39*, 4555. (n) Magueres, P. L.; Hubig, S. M.; Lindeman, S. V.; Veya, P.; Kochi, J. K. *J. Am. Chem. Soc.* **2000**, *122*, 10073. (o) Ara, I.; Fornies, J.; Gomez, J.; Lalinde, E.; Moreno, M. T. *Organometallics* **2000**, *19*, 3137. (p) Wiechert, D.; Mootz, D.; Dahlems, T. *J. Am. Chem. Soc.* **1997**, *119*, 12665. (q) Chou, C.-C.; Su, C.-C.; Tsai, H.-L.; Lii, K.-H. *Inorg. Chem.* **2005**, *44*, 628. (r) Palaniandavar, M.; Butcher, R. J.; Addison, A. W. *Inorg. Chem.* **1996**, *35*, 467. (s) Holz, R. C.; Thompson, L. C. *Inorg. Chem.* **1993**, *32*, 5251. (t) Jones, P.; Vagg, R. S.; Williams, P. A. *Inorg. Chem.* **1984**, *23*, 4110. (v) Evans, W. J.; Boyle, T. J.; Ziller, J. W. *Inorg. Chem.* **1992**, *31*, 1120.

© 2009 American Chemical Society
Published on Web 5/6/2009

Scheme 1

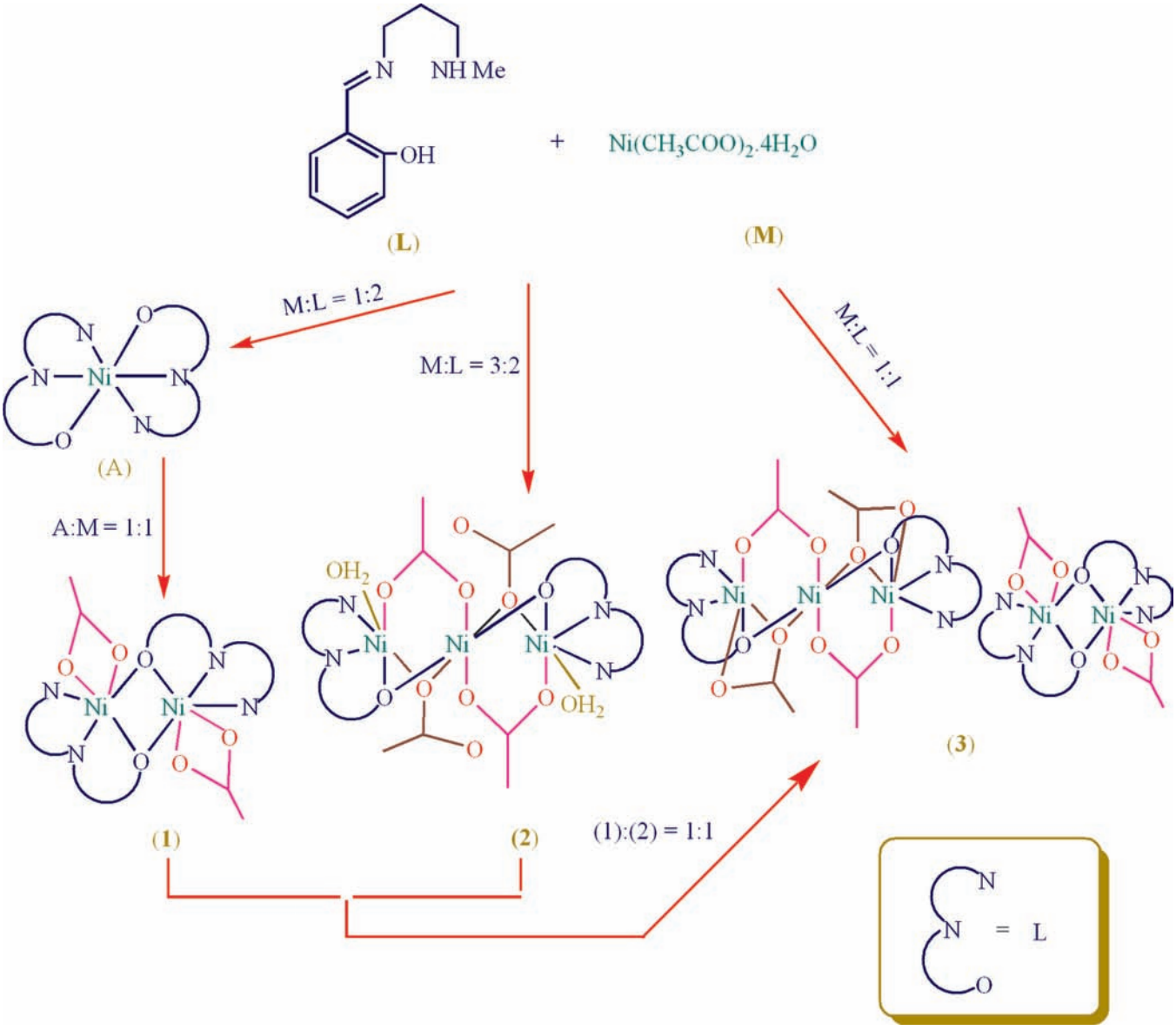

are (1) structural similarity, (2) similar potential energies, and (3) almost similar crystallization kinetics.[7] Among the reported organic cocrystals, most of them are acid−base compounds.[2a−2i] However, cocrystals containing only metal complexes are relatively rare,[2j−2v] because of the fact that compounds with different geometries rarely possess similar lattice packing forces and exhibit similar crystallization kinetics. The interest in organic (mostly pharmaceuticals) cocrystals stems mostly from the fact that cocrystallization may lead to significant improvement in certain properties,[8] for example, physical stability, solubility, bioavailability, processability, drug plasma concentration, etc.,[2c,8] as compared to the respective pure active components. However, unlike their organic counterpart, almost all the reported inorganic cocrystals are accidental products, and to the best of our knowledge, no attempts were taken until now to separate the individual components in order to compare their structure and properties in their free form and in the cocrystal. Crystallization of the individual components is also important for understanding the governing factors of cocrystallization and in turn for the design of new systems.

Herein, we report the synthesis and crystal structure of a 1:1 cocrystal of the dinuclear and trinuclear complexes formed by the Schiff base ligand 2-[(3-methylamino-propylimino)-methyl]-phenol (HL) (Scheme 1) with Ni(II) acetate. Both the dinuclear and trinuclear species have also been synthesized and crystallized separately and characterized structurally and magnetically.

The design of molecule-based magnets with polynuclear transition metal complexes relies on the presence of

(3) McMahon, J. A.; Bis, J. A.; Vishweshwar, P.; Shattock, T. R.; McLaughlin, O. L.; Zaworotko, M. J. *Z. Kristallogr.* **2005**, *220*, 340.
(4) Almarsson, O.; Zaworotko, M. J. *Chem. Commun.* **2004**, *17* 1889.
(5) Wöhler, F. *Annalen* **1844**, *51*, 153.
(6) Allen, F. H. *Acta Crystallogr., Sect. B* **2002**, *58*, 380.
(7) Datta, J.; Nandi, A. K. *Polymer* **1994**, *35*, 4804.
(8) Variankaval, N.; Wenslow, R.; Murry, J.; Hartman, R.; Helmy, R.; Kwong, E.; Clas, S.; Dalton, C.; Santos, I. *Cryst. Growth Des.* **2006**, *6*, 690–700.

both intra- and intermolecular coupling.[9] Since there are many structural parameters that may govern the magnetic exchange in these metal complexes, a first step in order to better understand the structural features that correlate with the strength and sign of the magnetic interaction is the preparation and characterization of metal complexes presenting subtle structural changes. From the study of the magnetic properties of these complexes, it may be possible to infer the key structural parameters that control the magnetic interaction in order to rationally design new complexes with the desired properties. These necessary magneto-structural correlations can be easily obtained if we are able to isolate and crystallize a given metallic complex in closely related environments, leading to subtle changes in the structure and properties. The isolation of dinuclear and trinuclear Ni(II) complexes as well as their cocrystals provides a very good opportunity for studying the magnetic properties of these complexes with slightly different crystal environments. This study reveals similar antiferromagnetic couplings within the Ni(II) dimers but different behavior within the trimers (weak antiferromagnetic coupling in the free form and weak ferromagnetic coupling in the cocrystal, due to minor changes in the coordination geometries). To the best of our knowledge, this is the first report of an inorganic coordination compound where both the individual components and their cocrystals have been structurally and magnetically characterized.

Experimental Section

Materials. The reagents and solvents used were of commercially available reagent quality, unless otherwise stated.

Synthesis of the Schiff-Base Ligand 2-[(3-Methylaminopropylimino)-methyl]-phenol (HL) and the Complex [NiL$_2$]. The Schiff base was prepared by the condensation of salicylaldehyde (1.05 mL, 10 mmol) and N-methyl-1,3-propanediamine (1.04 mL, 10 mmol) in methanol (10 mL) as reported earlier.[10] Complex [NiL$_2$] was prepared by following the previously reported procedure.[11]

Synthesis of [Ni$_2$(L)$_2$(OAc)$_2$] (1). Ni(OAc)$_2\cdot$4H$_2$O (1.240 g, 5 mmol), dissolved in 10 mL of hot methanol, was added to a suspension of complex [NiL$_2$] (2.201 g, 5 mmol) in methanol (10 mL) with constant stirring. The color of the solution turned to light green, and a green precipitate separated out slowly on keeping the mixture at room temperature for several hours. The green solid was then filtered and washed with diethyl ether and then redissolved in a CH$_3$CN/CH$_2$Cl$_2$ (1:1 v/v) solvent mixture. The solution was left to stand overnight in the air, resulting in the precipitation of light green, X-ray-quality single crystals of complex **1** after slow evaporation of the solvent. Yield: 1.76 g; 80%. Anal. calcd for C$_{26}$H$_{36}$N$_4$Ni$_2$O$_6$: C, 50.53; H, 5.87; N, 9.07. Found: C, 50.42; H, 5.79; N, 9.15. IR (KBr pellet, cm^{-1}): 3303 ν(NH), 1646 ν(C=N), 1555 ν_{as}(C=O), 1442 ν_s(C=O). λ_{max} (solid, reflectance): 570, 932 nm.

Synthesis of [Ni$_3$(L)$_2$(OAc)$_4$(H$_2$O)$_2$]$\cdot$CH$_2$Cl$_2\cdot$2CH$_3$OH (2). Ni(OAc)$_2\cdot$4H$_2$O (1.860 g, 7.5 mmol), dissolved in 10 mL of hot methanol, was added to a methanolic solution (10 mL) of the ligand (HL; 5 mmol) and stirred for ca. 10 min. The color of the solution turned to deep green, and a green precipitate separated out within an hour. The green solid was then filtered and washed with diethyl ether and redissolved in a CH$_3$CN/CH$_2$Cl$_2$ (1:1 v/v) solvent mixture. The solution was left to stand overnight in the air, resulting in the precipitation of deep green, X-ray-quality single crystals of complex **2** after slow evaporation of the solvent. Yield: 2.09 g; 75%. Anal. calcd for C$_{33}$H$_{56}$N$_4$Ni$_3$O$_{14}$Cl$_2$: C, 40.45; H, 5.76; N, 5.72. Found: C, 40.25; H, 5.79; N, 5.90. IR (KBr pellet, cm^{-1}): 3413 ν(NH), 1637 ν(C=N), 1583 ν_{as}(C=O), 1471 ν_s(C=O). λ_{max} (solid, reflectance): 575 and 930 nm.

Synthesis of {[Ni(L)(OAc)]$_2$[Ni$_3$(L)$_2$(OAc)$_4$]}$\cdot$2CH$_3$CN (3). A methanolic solution (5 mL) of Ni(OAc)$_2\cdot$4H$_2$O (1.240 g, 5 mmol) was mixed with a methanolic solution (5 mL) of the ligand (HL; 5 mmol) and stirred for ca. 10 min. Upon standing the mixture overnight in an open atmosphere, a green precipitate with some straw-yellow-colored compound, [NiL$_2$], separated out. The solid was then filtered and washed with diethyl ether and then redissolved in CH$_3$CN (20 mL). The yellow compound [NiL$_2$], being less soluble, remained mostly undissolved and was separated by filtration. The solution was left to stand in the air to decrease the volume to about 5 mL, and the deep green crystalline compound that precipitated out was collected. The IR spectra and elemental analyses of this compound revealed that probably a minute amount of the dinuclear compound is present as an impurity. Therefore, it was recrystallized from MeCN twice more to obtain pure compound **3**, as confirmed by elemental analysis. The crystalline compound was redissolved in CH$_3$CN. Layering of the green solution with diethyl ether gave well-formed X-ray-quality deep-green single crystals of **3**. Yield: 0.59 g; 40%. Anal. calcd for C$_{60}$H$_{84}$N$_{10}$Ni$_5$O$_{16}$: C, 48.21; H, 5.66; N, 9.37. Found: C, 48.32; H, 5.59; N, 9.25. IR (KBr pellet, cm^{-1}): 3429 (broad) ν(OH), 1642 ν(C=N), 1558 ν_{as}(C=O), 1439 ν_s(C=O). λ_{max} (solid, reflectance): 570 and 928 nm.

Alternative Method for the Synthesis of the Cocrystal (3). The cocrystal (**3**) has also been synthesized by mixing the methanol solutions (10 mL each) of **1** (0.618 g, 1 mmol) and **2** (0.979 g, 1 mmol) and letting the solvent slowly evaporate at ambient temperature. When the volume of the solution became about 5 mL, the crystalline product of **3** was collected (yield: 0.96 g; 65%).

Physical Measurements. Elemental analyses (C, H, and N) were performed using a Perkin-Elmer 240C elemental analyzer. IR spectra in KBr (4500−500 cm^{-1}) were recorded using a Perkin-Elmer RXI FT-IR spectrophotometer. Electronic spectra (1500−250 nm) were recorded on a Hitachi U-3501 spectrophotometer. High-resolution mass spectra (HRMS) electrospray ionization (ESI) were recorded on a Qtof Micro YA263 high-resolution mass spectrometer. For HRMS (ESI), the sample was taken in CH$_3$OH. Variable-temperature susceptibility measurements were carried out in the temperature range 2−300 K with an applied magnetic field of 0.1 T on polycrystalline samples of the three compounds (with masses of 62.44, 35.54, and 39.61 mg for compounds **1**−**3**, respectively) with a Quantum Design MPMS-XL-5 SQUID magnetometer. The isothermal magnetizations were made at 2 K with magnetic fields of up to 5 T. The susceptibility data were corrected for the sample holder previously measured using the same conditions, for the diamagnetic contributions of the salt as deduced by using Pascal's constant tables (χ_{dia} = -356.2×10^{-6}, -539.4×10^{-6}, and -846.8×10^{-6} emu.mol^{-1} for **1**, **2**, and **3**, respectively), and for the temperature-independent paramagnetism of the Ni(II) ions (Nα = 120 emu$\cdot$mol^{-1} per Ni(II) ion).

Crystal Data Collection and Refinement. Crystal data for the three crystals are given in Table 1. A total of 3687, 6445, and 9156 independent data were collected with Mo Kα radiation at 150(2)K using the Oxford Diffraction X-Calibur CCD System for complexes **1**, **2**, and **3**, respectively. The crystals were positioned at 50 mm from the CCD. A total of 321 frames were measured with a counting time of 10 s. Data analysis was carried

(9) Kahn, O., *Molecular Magnetism*; VCH: New York, 1993.
(10) Hamalainen, R.; Ahlgren, M.; Turpeinen, U. *Acta Crystallogr., Sect. B* **1982**, *38*, 1577.
(11) Mukherjee, P.; Drew, M. G. B.; Estrader, M.; Ghosh, A. *Inorg. Chem.* **2008**, *47*, 7784.

Table 1. Crystal Data and Structure Refinement of Complexes **1**, **2**, and **3**

	1	**2**	**3**
empirical formula	$C_{26}H_{36}N_4Ni_2O_6$	$C_{33}H_{56}N_4Ni_3O_{14}Cl_2$	$C_{60}H_{84}N_{10}Ni_5O_{16}$
fw	617.97	979.79	1494.82
space group	$P2_1/c$	$P2_1/c$	$P\bar{1}$
cryst syst	monoclinic	monoclinic	triclinic
a/Å	10.056(5)	10.4256(3)	10.2053(11)
b/Å	16.355(3)	20.4513(7)	12.4950(12)
c/Å	8.5705(7)	10.8823(3)	13.3825(13)
α/deg	90	90	104.438(9)
β/deg	103.77(2)	105.031(3)	90.042(8)
ν/deg	90	90	96.835(8)
V/Å^3	1369.0(7)	2240.91(12)	1640.0(3)
Z, calcd density	2, 1.499 g/cm^3	2, 1.452 g/cm^3	1, 1.514 g/cm^3
abs coeff (μ) mm^{-1}	1.422 (Mo Kα)	1.429 (Mo Kα)	1.482 (MoKa)
F(000)	648	1024	782
cryst size	0.02 × 0.03 × 0.20	0.04 × 0.04 × 0.27	0.05 × 0.05 × 0.30
refinement method	SHELXL-97 on F^2	SHELXL-97 on F^2	SHELXL-97 on F^2
θ range for data collection	2.43−30.0°	2.61−30.0°	2.47−30.0°
R(int)	0.040	0.028	0.077
no. of unique data	3687	6445	9156
no. of data with $I > 2\sigma(I)$	2218	4901	4765
R1, wR2	0.0600, 0.1447	0.0548, 0.1443	0.0592, 0.1514
goodness-of-fit on F^2	0.928	1.140	0.921

out with the Crysalis program.[12] The structures were solved using direct methods with the Shelx97 program.[13] The non-hydrogen atoms were refined with anisotropic thermal parameters. The hydrogen atoms bonded to carbon and nitrogen were included in geometric positions and given thermal parameters equivalent to 1.2 times those of the atom to which they were attached. Hydrogen atoms on the water molecule in **2** were located in a difference Fourier map and refined with distance constraints. Complex **2** contains solvent dichloromethane, refined with 50% occupancy, and a methanol molecule refined with full occupancy. Complex **3** contains solvent acetonitrile molecules. Absorption corrections were carried out using the ABSPACK program.[14] The structures were refined on F^2 using Shelx97[13] to R1 = 0.0600, 0.0548, and 0.0592 and wR2 = 0.1332, 0.1358, and 0.1387 for 2217, 4901, and 4765 reflections above the background with $I > 2\sigma(I)$ for compounds **1**−**3**, respectively.

Results and Discussion

Synthesis of the Complexes. The addition of a methanol solution of $Ni(OAc)_2$ to a methanol solution of the ligand (HL) in a 1:1 molar ratio resulted in the formation of a deep green cocrystal of $\{[Ni(L)(OAc)]_2[Ni_3(L)_2(OAc)_4]\}$ (**3**) along with a very small amount of the free dinuclear compound **1** and the bis complex $[NiL_2]$. After recrystallization (at least three times) of this mixture from acetonitrile, cocrystals of compound **3** were obtained in the pure form, as confirmed by elemental analysis. The individual components of the cocrystal, the dinuclear and trinuclear compounds, have also been synthesized by changing the reaction procedure. Increasing the Ni/L ratio leads to the formation of mixtures of the cocrystal (**3**) and the free trinuclear compound (**2**) with increasing proportions of the free trinuclear compound. Finally, when the Ni/L ratio reached 3:2, the pure free trinuclear compound (**2**) was obtained. If we look at the M/L compositions of the dinuclear (**1**) and trinuclear (**2**) compounds (1:1 and 3:2, respectively), we may think that a decrease in the Ni/L ratio should favor the formation of the dinuclear compound (**1**) in the pure form. Nevertheless, all of the attempts to prepare the free dinuclear compound by reducing the Ni/L ratio failed, and when the Ni/L ratio is kept between 1:1 and 1:2, a mixture of the cocrystal (**3**), the free dinuclear compound **1**, and the bis complex $[NiL_2]$ resulted. Unfortunately, this mixture contains a very small amount of **1**, and we failed to get it in pure form by recrystallization. On further lowering the Ni/L ratio to less than 1:2, the bis complex $[NiL_2]$ became the only product. All of the results show that the cocrystal (**3**) is one of the products when the Ni/L ratio is kept between 1:2 and 3:2. The isolation of cocrystals requires the presence of both dinuclear and trinuclear species in solution. Thus, the trinuclear species is formed even when the Ni/L ratio is 1:1 (the stoichiometry of the dinuclear compound) or less. We investigated the species distribution in solutions by HRMS (ESI) spectra (Figures S1−S5, Supporting Information) and found the presence of trinuclear species (HRMS (ESI) found: m/z $(M + Na)^+ = 853.8030$; $(M + Na)_{calcd}^+ = 853.79$, where M = molecular weight of the trinuclear unit) until the Ni/L became less than 1:2 (when only $[NiL_2]$ is formed, HRMS (ESI) found: m/z $(M + Na)^+ = 464.3425$; $(M + Na)_{calcd}^+ = 464.19$). The HRMS (ESI) data show that the dinuclear species (HRMS (ESI) found: m/z $(M + Na)^+ = 641.5192$; $(M + Na)_{calcd}^+ = 641.09$) is also formed in this range of Ni/L ratios, but interestingly, its peak intensity became negligible when the Ni/L was 3:2. The electronic spectral data (Figure S6−S10, Supporting Information) also show that, upon increasing the proportion of metal salt, the spectrum gradually changes to be the same as that of the pure trinuclear species. All of these results clearly show that the trinuclear compound (**2**) is theromodynamically more stable when the Ni/L is 3:2 and isolated from the solution as a cocrystal when compound **1** is also present. During the synthesis of the complexes by the addition of free ligand to the metal salt, the formation of different species may take place in the solution due to the presence of a local excess of metal ions (or ligand), and the

(12) *Crysalis*, v. 1; Oxford Diffraction Ltd.: Oxford, U.K., 2005.
(13) Sheldrick, G. M. *SHELXL-97*; University of Göttingen: Göttingen, Germany, 1997.
(14) *ABSPACK*; Oxford Diffraction Ltd: Oxford, U.K., 2005.

solubility of the products plays a very important role in the isolation of the compounds in the solid state. For the synthesis of the dinuclear complex (**1**) in pure form, we adopt a procedure that avoids the presence of any local excess of Ni(II) and consequently prevent the formation of the trinuclear complex. Thus, we first synthesized the bis complex $[NiL_2]$ by reacting nickel acetate and the ligand in a 1:2 molar ratio. A suspension of this complex in methanol was then reacted at room temperature with a methanolic solution of $Ni(OAc)_2 \cdot 4H_2O$ in a 1:1 molar ratio to yield the pure dinuclear compound (**1**). As expected, an increase in the proportion of the metal salt leads to the formation of the cocrystal (**3**) along with the dinuclear and trinuclear complexes. Finally, when the Ni/NiL_2 ratio became 2:1 (i.e., the Ni/L ratio became 3:2), the pure trinuclear compound (**2**) was obtained. The synthesis of the cocrystal **3** by mixing up the dinuclear and trinuclear compounds (**1** and **2**, respectively) clearly demonstrates that the solubility of compound **3** is lower than those of the individual precursor complexes, as also observed in the alum salts, $M^{I}M^{III}(SO_4)_2 \cdot 12H_2O$, which are less soluble than the corresponding $M^{I}_2(SO_4)$ and $M^{III}_2(SO_4)_3$ salts.

IR and UV−Vis Spectra of Complexes. In the IR spectra of complexes **1**, **2**, and the cocrystal **3**, a sharp band around 3300 cm^{-1} is observed due to NH stretching. For complex **2**, an additional broad band centered at 3413 cm^{-1} is due to the ν(OH) of water and methanol. The attributions of the IR spectra in the 1300−1650 cm^{-1} region are difficult due to the appearance of several absorption bands from both the Schiff base and the acetate ligands. However, by comparing the IR spectra of the Ni(II) complexes of the same ligand but with other anions (NO_3^- and halides), the moderately strong and sharp band at 1646, 1637, and 1642 cm^{-1}, respectively, for **1**−**3** are assigned to the azomethine ν(C=N) group. The strong bands at 1555, 1583, and 1558 cm^{-1} are likely due to the antisymmetric stretching mode of the carboxylate group and the bands at 1415, 1420, and 1439 cm^{-1} to the symmetric stretching modes of the carboxylates.[15]

The solid-state reflectance spectra of all of the complexes show a broad band at ca. 930 nm, well separated from a second transition at ca. 570 nm, as usually observed in octahedral Ni(II) complexes.[11,16] The higher energy d−d bands are obscured by strong charge-transfer transitions.

Description of the Structures

The metal atoms in all three structures exhibit slightly distorted six-coordinated octahedral environments. Complex **1** is a centrosymmetric nickel dimer $[Ni_2L_2(OAc)_2]$, while **2** is a centrosymmetric trinuclear nickel compound, $[(Ni_3L_2(OAc))_3(H_2O)_2]$. On the other hand, **3** contains the same centrosymmetric nickel dimer $[Ni_2L_2(OAc)_2]$ as in **1** and a centrosymmetric trinuclear nickel complex $[Ni_3(L)_2(OAc)_4]$ very similar to that found in **2**. The bond distances and angles in the two complexes in **3** are very similar to those found separately in **1** and **2**.

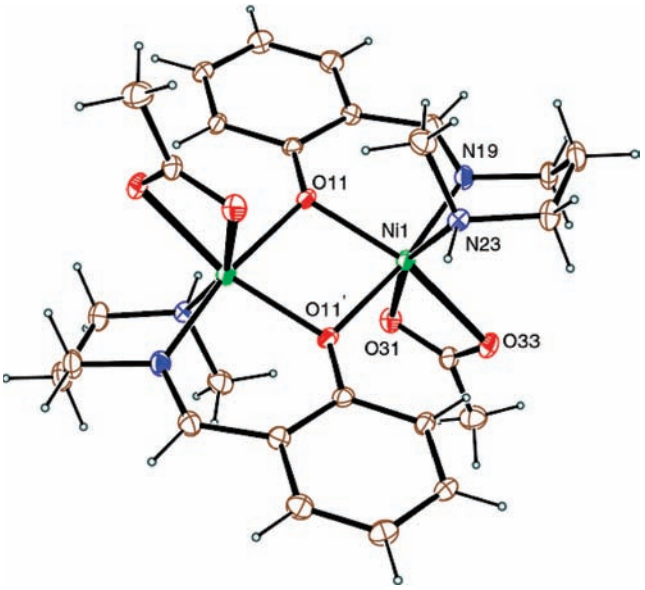

Figure 1. ORTEP-3 view of the asymmetric unit of **1** with ellipsoids at 30% probability.

$[Ni_2L_2(OAc)_2]$ (1). The crystal structure of **1** contains a discrete centrosymmetric dimeric unit containing the neutral complex $[Ni_2L_2(OAc)_2]$ (Figure 1). Selected bond lengths and angles are summarized in Table 2. The dinuclear unit is formed by two Ni(II) atoms labeled Ni(1) and Ni(1′) (′ = 2 − x, 2 − y, −z), bridged by the two μ_2-phenoxo oxygen atoms O(11) and O(11′) of the Schiff-base ligands. The metal atom Ni(1) has a distorted octahedral environment, being coordinated by an amine nitrogen, N(23); an imine nitrogen, N(19); a chelated acetate ligand via the oxygen atoms O(31) and O(33); and two phenoxo oxygen atoms, O(11) and O(11′), of the tridentate ligands that bridge the two Ni(II) ions within the dimer. The three donor atoms of the tridentate Schiff base coordinate in a *fac* configuration to the Ni(II) ions. The $Ni-O_{phe}$, $Ni-N_{imi}$, and $Ni-N_{ami}$ bond distances are 2.018(3), 2.012(3), and 2.078(3) Å, respectively, in good agreement with those observed for similar compounds in the literature.[16] As usually found in oxo-bridged Ni(II) complexes, the bridging Ni−O(11′) bond length (2.109(2) Å) is slightly longer than the chelating Ni−O(11) bond distance (2.018(3) Å). The distance between the two Ni atoms is 3.176(4) Å, indicating the absence of any bond between the two nickel centers. The Ni−O11−Ni′ bridge angle is 100.58(10)°. A rather unusual feature of the complex is the *fac* configuration of the Schiff base ligand. There are several reports[16] of a double phenoxo-bridged Ni(II) dimer with tridentate ligands, but in most of them, the ligands are coordinated in a *mer* configuration. The chelating coordination of the acetate coligand that must span cis positions seems to be responsible for the *fac* coordination of the Schiff base ligand L with a folded conformation.

$[Ni_3(L)_2(OAc)_4(H_2O)_2] \cdot CH_2Cl_2 \cdot 2CH_3OH$ (2). The crystal structure of **2** consists of a discrete trinuclear unit containing the neutral complex $[Ni_3(L)_2(OAc)_4(H_2O)_2]$, together with one CH_2Cl_2 and two CH_3OH solvent molecules (Figure 2). Selected bond lengths and angles

(15) Costes, J. P.; Dahan, F.; Laurent, J. P. *Inorg. Chem.* **1985**, *24*, 1018 and references cited therin.

(16) (a) Dey, M.; Rao, C. P.; Saarenketo, P. K.; Rissanen, K. *Inorg. Chem. Commun.* **2002**, *5*, 924. (b) Koizumi, S.; Nihei, M.; Oshio, H. *Chem. Lett.* **2003**, *32*, 812. (c) Banerjee, S.; Drew, M. G. B.; Lu, C.-Z.; Tercero, J.; Diaz, C.; Ghosh, A. *Eur. J. Inorg. Chem.* **2005**, 2376 and references cited therein.

Table 2. Bond Distances (Å) and Angles (deg) of the Ni(II) Dimers in Compounds **1** and **3**[a]

bond	**1**	**3A**
Ni(1)−O(31)	2.172(3)	2.185(3)
Ni(1)−O(11)	2.018(3)	2.025(3)
Ni(1)−O(11)′	2.109(2)	2.099(3)
Ni(1)−O(33)	2.118(3)	2.109(3)
Ni(1)−N(19)	2.012(3)	2.025(3)
Ni(1)−N(23)	2.078(3)	2.099(3)
angle	**1**	**3A**
N(19)−Ni(1)−O(11)	91.52(11)	89.99(12)
N(19)−Ni(1)−N(23)	86.88(12)	86.94(13)
O(11)−Ni(1)−N(23)	101.56(11)	103.21(12)
N(19)−Ni(1)−O(11)′	170.41(11)	170.29(12)
O(11)−Ni(1)−O(11)′	79.41(10)	80.61(11)
N(23)−Ni(1)−O(11)′	91.87(11)	92.82(12)
N(19)−Ni(1)−O(33)	92.73(11)	92.07(12)
O(11)−Ni(1)−O(33)	158.76(10)	158.56(11)
N(23)−Ni(1)−O(33)	99.45(11)	98.20(12)
O(33)−Ni(1)−O(11)′	96.85(10)	97.57(10)
N(19)−Ni(1)−O(31)	91.22(11)	89.64(12)
O(11)−Ni(1)−O(31)	97.58(10)	97.28(11)
N(23)−Ni(1)−O(31)	160.80(11)	159.21(12)
O(31)−Ni(1)−O(11)′	93.04(9)	93.93(11)
O(33)−Ni(1)−O(31)	61.54(10)	61.41(11)
Ni(1)−O(11)−Ni(1)′	100.58(10)	99.39(11)

[a] Symmetry code (′) = $2-x, 2-y, -z$ in **1** and $1-x, -y, 2-z$ in **3A**.

are summarized in Table 3. In the trinuclear complex, the three Ni atoms are six-coordinate with a distorted octahedral environment, and the Ni_3 unit is perfectly linear, owing to the presence of a crystallographic inversion center at the central nickel atom Ni(1). Each of the two terminal nickel atoms, Ni(2), are coordinated by the two nitrogen atoms (N(19) and N(23)) and a phenoxo oxygen atom, O(11), of the deprotonated Schiff base ligand (L), one oxygen atom, O(31), of a bridging monodentate acetate, another oxygen atom, O(41), of a bridging bidentate acetate, and an oxygen atom, O(100), of a water molecule. The equatorial plane consists of the Schiff base coordinated in a *mer* configuration together with O(31). The equatorial bond lengths around the Ni(2) atom (Ni(2)−O(11), 2.037(2) Å; Ni(2)−O(31), 2.125(2) Å; Ni(2)−N(19), 2.043(2) Å; and Ni(2)−N(23), 2.109(3) Å) are similar to the axial ones (Ni(2)−O(41), 2.053(2) Å and Ni(2)−O(100), 2.121(2) Å). The deviations of the four basal donor atoms from their mean plane are within ±0.042 Å. The Ni atom deviates from the mean plane by 0.030(4) Å. The six-membered ring comprising the nickel, imine N atoms, three propylene C atoms, and amino N atom adopts a screw-boat conformation, while that containing the aromatic moiety adopts an envelope conformation.

The central Ni(1) sits on an inversion center and presents a distorted octahedral coordination involving two bridging phenoxo oxygen atoms, O(11) and O(11′), from two terminal units and two oxygen atoms, O(43) and O(43′), from each of the two bridging bidentate acetate groups constituting the equatorial plane. The apical positions are occupied by O(31) and O(31′) of the bridging monodentate (1:2κO) acetate ligand. The Ni(1)−O bond lengths range from 2.066(2) to 2.085(2) Å, the shortest bond being to the phenoxo O atom of the ligand. The distance between the Ni(1) and Ni(2) atoms is

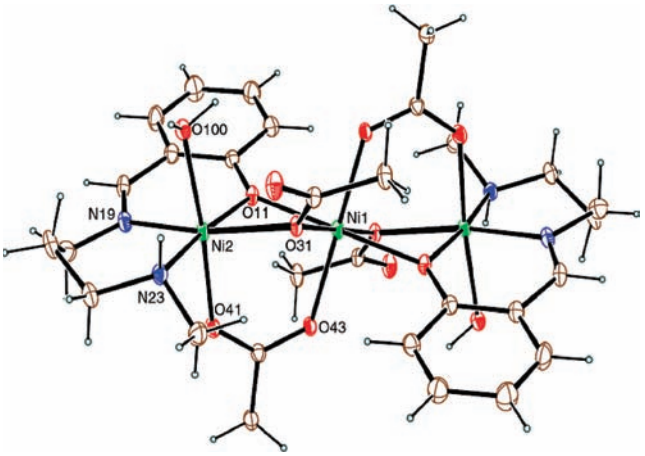

Figure 2. ORTEP-3 view of the asymmetric unit of **2** with ellipsoids at 30% probability.

Table 3. Bond Distances (Å) and Angles (deg) of the Ni(II) Trimers in Compounds **2** and **3**

bond	**2** (X = 100)	**3B** (X = 33)
Ni(1)−O(11)	2.065(2)	2.048(2)
Ni(1)−O(31)	2.085(2)	2.123(3)
Ni(1)−O(43)	2.072(2)	2.045(3)
Ni(2)−N(19)	2.043(3)	2.018(3)
Ni(2)−N(23)	2.110(3)	2.102(3)
Ni(2)−O(11)	2.037(2)	2.019(3)
Ni(2)−O(31)	2.125(2)	2.137(2)
Ni(2)−O(X)	2.121(2)	2.183(3)
Ni(2)−O(41)	2.053(2)	2.023(3)
angle	**2** (X = 100)	**3B** (X = 33)
O(11)−Ni(1)−O(43)	91.58(9)	90.17(10)
O(11)−Ni(1)−O(31)	77.06(8)	80.31(10)
O(43)−Ni(1)−O(31)	90.33(9)	90.56(11)
O(11)−Ni(2)−N(19)	90.16(10)	91.04(12)
O(11)−Ni(2)−O(41)	91.07(9)	89.81(11)
N(19)−Ni(2)−O(41)	89.65(10)	98.88(12)
O(11)−Ni(2)−N(23)	171.91(10)	171.48(12)
N(19)−Ni(2)−N(23)	97.92(11)	97.46(13)
O(41)−Ni(2)−N(23)	88.63(10)	88.33(12)
O(11)−Ni(2)−O(X)	90.91(9)	91.64(11)
N(19)−Ni(2)−O(X)	85.31(10)	99.96(11)
O(41)−Ni(2)−O(X)	174.59(9)	161.07(10)
N(23)−Ni(2)−O(X)	90.11(10)	87.46(12)
O(11)−Ni(2)−O(31)	76.77(8)	80.60(10)
N(19)−Ni(2)−O(31)	166.31(10)	158.53(12)
O(41)−Ni(2)−O(31)	94.61(9)	100.81(10)
N(23)−Ni(2)−O(31)	95.19(10)	91.59(11)
O(X)−Ni(2)−O(31)	90.74(9)	60.89(10)
Ni(2)−O(11)−Ni(1)	99.89(9)	97.63(11)
Ni(2)−O(31)−Ni(1)	96.49(9)	91.87(10)

3.141(4) Å, indicating the absence of any bond between the two nickel centers. The Ni(2)−O(11)−Ni(1) and Ni(2)−O(31)−Ni(1) bridge angles are 99.89(9)° and 96.49(9)°. It should be noted that there are very few examples of similar trinuclear Ni(II) complexes bridged by both single-atom and bidentate acetate as well as a phenoxo (or oxo) group of the tridentate chelating ligand. Indeed, only two such compounds are reported with the reduced Schiff base ligands, N-(2-hydroxybenzyl)propanolamine[16] and 2-Methyl-2-(2-methyl-benzylamino)-propan-1-ol,[16] and it is proposed that the higher flexibility of the reduced Schiff base is responsible for the formation of the trinuclear complexes. The present complex is thus the first trinuclear compound of Ni(II) with such a bridging

system containing a Schiff base (nonreduced) ligand. Its isolation shows that reduction of the Schiff base is not essential for the synthesis of this type of trinuclear Ni(II) complexes.

Both hydrogen atoms of the water molecule O(100) are involved in hydrogen bonds (Table 4). One of them, H(1), forms a H bond with the O(51) atom of a methanol solvent molecule (H···O = 1.80 Å, O−H···O = 174°, and O···O = 2.662 Å). The other hydrogen atom, H(2), forms an intermolecular hydrogen bond with the uncoordinated oxygen atom of the bridging single-atom acetate group of a neighboring unit, O(33′) (′ = 1 − *x*, 1 − *y*, 1 − *z*; H···O = 1.91 Å, O−H···O = 170°, and O···O = 2.751 Å). These H bonds form an infinite 1-D hydrogen-bonded chain, as shown in Figure 3. The amine hydrogen atom H(23) participates in a relatively weak intramolecular hydrogen bond to the uncoordinated oxygen, O(33), of the bridging monodentate acetate ligand of the same unit (H···O = 2.51 Å, N−H···O = 116°, and N···O = 3.025 Å) as well as in an intermolecular hydrogen bond to O(33′) (′ = 1 − *x*, 1 − *y*, 1 − *z*) of the neighboring unit (H···O = 2.31 Å, N−H···O = 154°, and N···O = 3.151 Å).

Table 4. Hydrogen-Bond Parameters in Compound **2** (in Å and deg)[a]

D−H···A	*d*(D−H)	*d*(D···A)	*d*(H···A)	<(D−H···A)
O100−H1···O51	0.87	2.66	1.80	168
O100−H2···O33′	0.86	2.75	1.91	168
N23−H23···O33	0.91	3.03	2.51	116
N23−H23···O33′	0.91	3.15	2.31	154
O51−H51···O43″	0.82	2.72	1.90	172

[a] Symmetry code (′) = (1 − *x*, 1 − *y*, 1 − *z*), (″) = (−*x*, 1 − *y*, 1 − *z*).

{[Ni(L)(OAc)]$_2$[Ni$_3$(L)$_2$(OAc)$_4$]}·2CH$_3$CN (3). The molecular structure of the cocrystal complex **3** contains a discrete dinuclear complex (named **3A**) and a discrete trinuclear complex [Ni$_3$(L)$_2$(OAc)$_4$] (named **3B**), together with one CH$_3$CN solvent molecule (Figure 4). Selected bond lengths and angles are summarized in Tables 2 and 3 for units **3A** and **3B**, respectively. The most important and original aspect of the structure of compound **3** is that the dimeric unit **3A** is equivalent to the dimeric complex found in **1**, while the structure of the trimeric unit **3B** is almost identical to the trimeric complex found in compound **2**. That is, it can be considered as the cocrystal of **1** and **2**. The only difference between the two trimers is the presence of a coordinated water molecule in complex **2**, which is replaced by the second oxygen atom, O(33b), from the bridging acetate ligand that connects the terminal nickel atoms to the central one through O(31b) in a $1\kappa^2OO':2\kappa O$ manner (Figure 5).

The intradimer bond lengths and angles in **1** and **3A** are equivalent (Table 2). Thus, the Ni−L ligand bond distances are very similar in both complexes (Ni(1)−O(11) = 2.018(3), 2.025(3) Å; Ni(1)−N(19) = 2.012(3), 2.025(3) Å; and Ni(1)−N(23) = 2.078(3), 2.099(3) Å, in complexes **1** and **3A**, respectively). In both complexes, the distance to the imino nitrogen N(19) is shorter than that to the amino nitrogen N(23). The Ni−O bond lengths to the

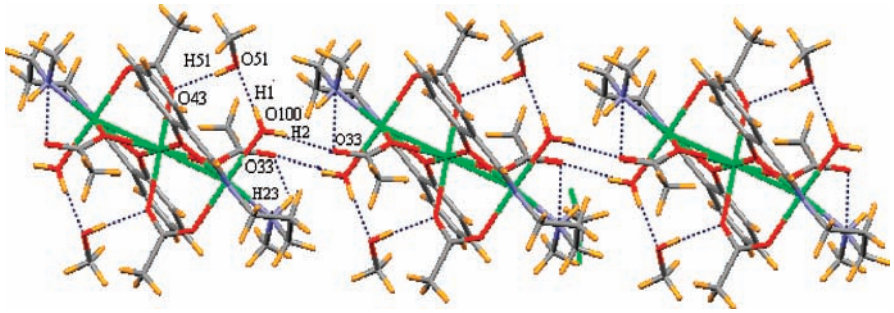

Figure 3. Hydrogen-bonded 1D chain of complex **2**. The intermolecular hydrogen bonds are shown as dashed lines; atoms marked with a (′) are transformed by the symmetry elements 1 − *x*, 1 − *y*, 1 − *z*

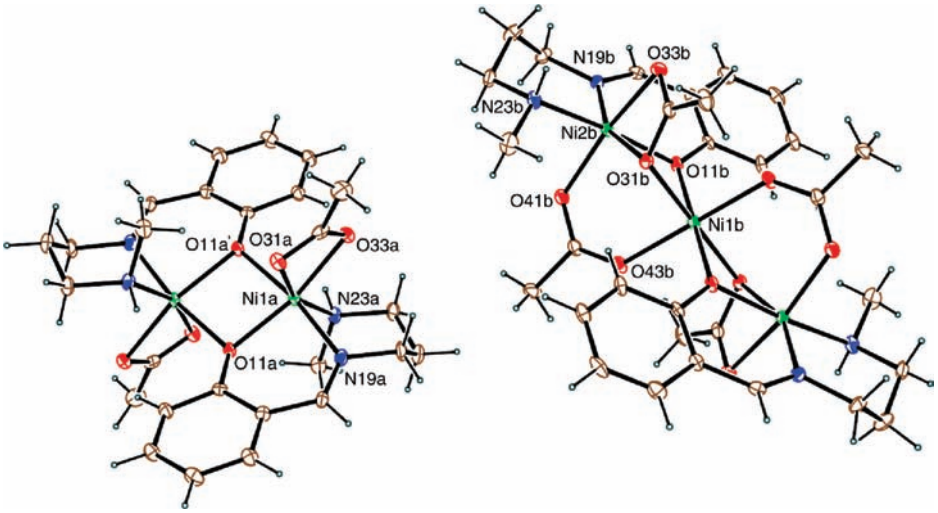

Figure 4. ORTEP-3 view of the asymmetric unit of **3** with ellipsoids at 25% probability.

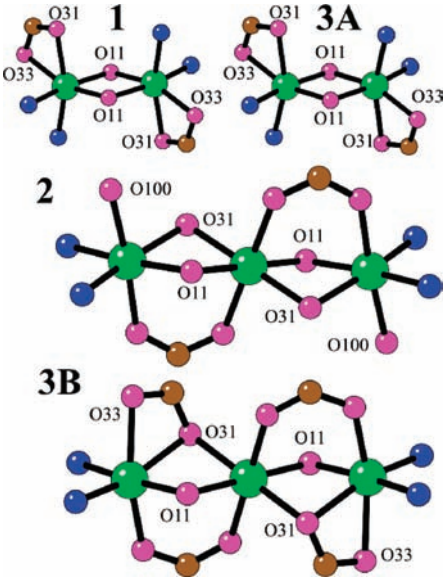

Figure 5. Comparison of the Ni(II) dimers and trimers in compounds **1** and **2** and in the cocrystal **3** (**3A** and **3B**) (color code: C = brown, O = pink, N = blue, and Ni = green).

bidentate acetate ligand for complexes **1** and **3A**, respectively, are 2.172(3) and 2.185(3) Å to O(31), which is trans to N(23), and 2.118(3) and 2.109(3) Å to O(33), which is trans to O(11), while the distances to O(11′) (′ = $2-x, 2-y, -z$) are 2.109(2) and 2.099(3) Å, respectively.

In the centrosymmetric Ni(II) trimers, the arrangement around the central Ni(1) is equivalent in **2** and **3B** with Ni(1)−O(11) = 2.065(2) and 2.048(2) Å, Ni(1)−O(31) = 2.085(2) and 2.123(3) Å, and Ni(1)O(43) = 2.072(2) and 2.045(3) Å in **2** and **3B**, respectively. For the terminal Ni(2) atoms, the replacement in the coordination sphere of the water molecule present in **2** by a second acetate oxygen atom, O(33), in **3B** gives rise to slight changes in the bond distances and angles. Thus, although the Ni−ligand bond distances are very similar in both complexes (Ni(2)−O(11) = 2.037(2), 2.019(3) Å; Ni(1)−N(19) = 2.043(3), 2.018(3) Å; and Ni(1)−N(23) = 2.110(3), 2.102(3) Å in **2** and **3B**, respectively), those to the acetate oxygen atoms O(31) and O(41) are slightly different (2.125(2) and 2.053(2) Å in **2** and 2.137(2) and 2.023(3) Å) in **3B**, but there are significant differences in the bond angles involving O(31) (Table 3). These differences between the bond lengths and angles are presumably due to the fact that the bridging modes of the acetate ligand to the nickel atom involving O(31) are different. The Ni−O(100) bond distance to the water molecule in complex **2** (2.121(2) Å) is shorter than that to the second acetate oxygen atom, O(33) (2.183(3) Å), in **3B**. In addition, the coordination sphere around the terminal Ni atoms in **3B** are more distorted than those found in **2** due to the presence of the chelated acetate ligand with a bite angle of 60.89(10)° (Table 3). Moreover, the Ni−O−Ni bond angles in compound **2** are significantly larger than those of the trinuclear complex (**3B**) in compound **3** (Table 3). The tridentate bridging mode of the acetate group ($1\kappa^2OO':2\kappa O'$) that is found in **3B** is rare in Ni(II) complexes but is found in some dinuclear Ni(II) complexes [17] and in one tetranuclear Ni(II) complex.[18] As far as we know, this is also the first example of a trinuclear Ni(II) complex with this bridging mode of acetate (Figure 5).

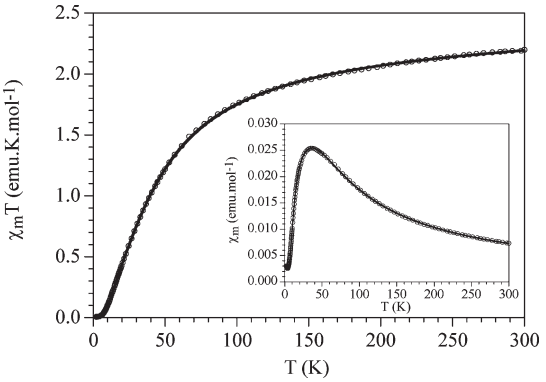

Figure 6. Thermal variation of the $\chi_m T$ product for compound **1**. Inset shows the thermal variation of the molar magnetic susceptibility (χ_m). Solid line represents the best fit to the model (see text).

Magnetic Properties. The thermal variation of the product of the molar magnetic susceptibility times the temperature ($\chi_m T$) per Ni(II) dimer for compound **1** shows at room temperature a value of 2.20 emu·K·mol^{-1}, close to the expected spin-only value for two isolated $S = 1$ Ni(II) ions (2.0 emu·K·mol^{-1}). When the sample is cooled, $\chi_m T$ shows a continuous decrease starting at room temperature, to reach a value of ca. 0 emu·K·mol^{-1} below ca. 5 K (Figure 6). This behavior indicates that compound **1** presents an antiferromagnetic Ni−Ni exchange coupling inside its dimeric structure. This antiferromagnetic coupling is confirmed by the thermal variation of the molar magnetic susceptibility, χ_m, that shows a rounded maximum at ca. 40 K (inset in Figure 6). Below this temperature, χ_m shows a sharp decrease and a very tiny increase at very low temperatures, arising from the presence of a small amount of paramagnetic monomeric Ni(II) impurities.

Since the structure of compound **1** shows the presence of well-isolated Ni(II) dimers connected through two oxo bridges, we have fitted the magnetic properties of this compound to a simple model of an $S = 1$ dimer with an additional paramagnetic $S = 1$ contribution to account for the tiny increase in the χ_m plot at very low temperatures:[19]

$$\chi_m = (1-c)\frac{Ng^2\beta^2}{kT}\frac{2e^{2x}+10e^{6x}}{1+3e^{2x}+5e^{6x}} + c\frac{2Ng^2\beta^2}{3kT}, \quad \text{with } x = J/\mathrm{kT} \qquad (1)$$

This simple model gives a very satisfactory fit of the magnetic properties of compound **1** in the whole

(17) (a) Adams, H.; Clunas, S.; Fenton, D. E.; Gregson, T. J.; McHugh, P. E.; Spey, S. E. *Inorg. Chim. Acta* **2003**, *346*, 239. (b) He, C.; Lippard, S. J. *J. Am. Chem. Soc.* **2000**, *122*, 184. (c) Wages, H. E.; Taft, K. L.; Lippard, S. J. *Inorg. Chem.* **1993**, *32*, 4985. (d) Sidorov, A. A.; Fomina, I. G.; Malkov, A. E.; Reshetnikov, A. V.; Aleksandrov, G. G.; Novotortsev, V. M.; Nefedov, S. E.; Eremenko, I. L. *Izv. Akad. Nauk SSSR, Ser. Khim. (Russ.) (Russ. Chem. Bull.)* **2000**, 1915.

(18) Reglinski, J.; Taylor, M. K.; Kennedy, A. R. *Inorg. Chem. Commun.* **2006**, *9*, 736.

(19) O'Connor, C. *J. Prog Inorg. Chem.* **1982**, *29*, 203.

temperature range with the following set of parameters: $g = 2.144(2)$, $2J = -36.18(7)$ K $= -25.14(5)$ cm^{-1}, and a paramagnetic $S = 1$ impurity of $c = 0.54\%$ (solid line in Figure 6; the Hamiltonian is written as $H = -2JS_1S_2$). Note that the magnetic coupling may also include a zero field splitting (ZFS) contribution, as is customarily observed in most Ni(II) complexes.[20] Nevertheless, attempts to fit the magnetic properties including both parameters lead to unreliable results since both parameters are strongly correlated.[20]

The thermal variation of the $\chi_m T$ product for compound **2** per Ni(II) trimer shows a room-temperature value of 3.48 emu·K·mol^{-1}, close to the expected spin-only value for three noninteracting $S = 1$ Ni(II) ions (3.0 emu·K·mol^{-1}). When the sample is cooled, the $\chi_m T$ product shows a smooth decrease from 300 to ca. 100 K that becomes more pronounced below ca. 100 K, to reach a smooth change of slope between ca. 10 and 5 K at a value of ca. 1.3 emu·K·mol^{-1} (Figure 7). Below ca. 5 K, $\chi_m T$ shows a more abrupt decrease to reach a value of ca. 1.0 emu·K·mol^{-1} at 2 K. This behavior indicates that compound **2** also presents antiferromagnetic exchange interactions inside the trinuclear Ni(II) complex. Unfortunately, this behavior cannot be confirmed in the thermal variation of the χ_m (not shown) for two reasons: the coupling is weaker than in compound **2** (see below), and the expected spin ground state of a linear trimer is paramagnetic ($S = 1$ in this case) since the three spins cannot be cancelled and, therefore, no maximum is observed in the thermal variation of the χ_m at low temperatures. The smooth change in the slope of the $\chi_m T$ plot at 5−10 K at a value of ca. 1.3 emu·K·mol^{-1} agrees with the presence of an $S = 1$ ground spin state for this compound (the isothermal magnetization also confirms this result, see below). Since the structure of compound **2** shows the presence of well-isolated centrosymmetric linear Ni(II) trimers, we have fitted the magnetic properties of this compound to the simple model derived for a centrosymmetrical $S = 1$ linear trimer with the Hamiltonian $H = -2J(S_1S_2 + S_2S_3)$, where S_2 is the spin state of the central Ni(II) ion:[21]

$$\chi_m = \frac{Ng^2\beta^2}{kT}\frac{28e^{4x} + 10e^{-2x} + 2e^{-6x} + 10e^{2x} + 2}{7e^{4x} + 8e^{-2x} + 3e^{-6x} + 5e^{2x} + e^{-4x} + 3}, \quad \text{with } x = J/\text{kT} \quad (2)$$

This simple model provides a very good fit of the experimental magnetic data over the whole temperature range with the following set of parameters: $g = 2.149(8)$ and $2J = -8.7(2)$ K $= -6.1(1)$ cm^{-1} (solid line in Figure 7). Note that this model is not able to reproduce the sharp decrease observed at very low temperatures (inset in Figure 7) probably because this decrease must be due to the presence of a ZFS in the $S = 1$ ground spin state. As also observed in compound **1**, attempts to fit both parameters (ZFS and antiferromagnetic coupling) result in unrealistic values since both factors are highly correlated and the magnetic coupling is weak.[22]

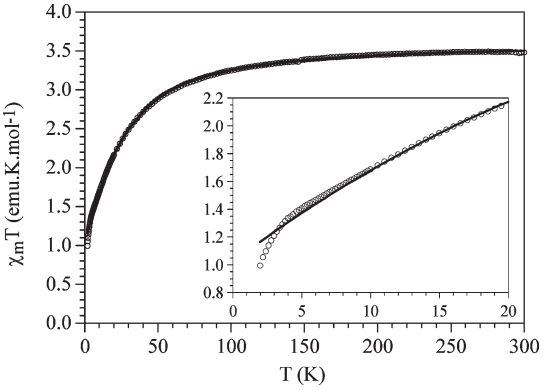

Figure 7. Thermal variation of the $\chi_m T$ product for compound **2**. Inset shows the low-temperature region. Solid line represents the best fit to the model (see text).

Compound **3** shows a $\chi_m T$ value at room temperature of 5.20 emu·K·mol^{-1} per formula unit, close to the expected spin only value for five noninteracting $S = 1$ Ni(II) ions (5.0 emu·K·mol^{-1}). When the temperature is decreased, $\chi_m T$ shows a very smooth decrease down to ca. 100 K and a more progressive decrease below this temperature (Figure 8). As in compound **2**, $\chi_m T$ shows a softening of the slope at low temperatures, although with a significantly higher $\chi_m T$ value (ca. 3.4 emu·K·mol^{-1}), suggesting the existence of a paramagnetic spin ground state (inset in Figure 8). At very low temperatures, $\chi_m T$ decreases more abruptly, to reach a value of ca. 2.7 emu·K·mol^{-1} at 2 K. As observed in compound **2**, this sharp decrease at very low temperatures may be attributed to the presence of a zero field splitting of the paramagnetic ground spin state. Since compound **3** is, from a structural point of view, a 1:1 mixture of compounds **1** (isolated Ni_2 complexes) and **2** (isolated Ni_3 complexes), it is straightforward to postulate that the magnetic properties of **3** must be the sum of those from **1** and **2** since both complexes also appear isolated in compound **3**. Accordingly, we have fitted the magnetic data of compound **3** with a model including an $S = 1$ dimer and a centrosymmetrical linear $S = 1$ trimer: $\chi_m = \chi_{dim} + \chi_{trim}$, where χ_{dim} and χ_{trim} are the corresponding values of an $S = 1$ dimer and centrosymmetrical lineal trimer, respectively (eqs 1 and 2). For simplicity, we have assumed that all the Ni(II) ions in both complexes have the same g factor. This model reproduces very satisfactorily the experimental data in the whole temperature range with the following set of parameters: $g = 2.0590(7)$, $2J_{dim} = 29.5(1)$ K $= 20.5(1)$ cm^{-1}, and $2J_{trim} = 0.23(1)$ K $= 0.16(1)$ cm^{-1} (solid line in Figure 8). Note that, as in compound **2**, the theoretical model does not reproduce the sharp decrease observed below ca. 5 K since this decrease must also be attributed to the ZFS of the $S = 3$ ground spin state of the trinuclear complex.[20]

An additional proof of the magnetic coupling present in these compounds and of their ground spin states is provided by the isothermal magnetizations at 2 K. Thus, compound **1** presents a very low magnetization at 2 K with a value of only 0.006 μ_B at 5 T (Figure 9), coming from a very low residual paramagnetic monomeric impurity, as also observed in the $\chi_m T$ plot. Com-

(20) Boca, R. *Coord. Chem. Rev.* **2004**, *248*, 757.
(21) (a) Rietmeijer, F. J.; Van Albada, G. A.; Graaff, R. A. G.; Haasnoot, J. G.; Reedijk, J. *Inorg. Chem.* **1985**, *24*, 3597. (b) Carlin, R. L. *Magnetochemistry*; Springer: Berlin, 1986.
(22) Zhang, W.; Bruda, S.; Landee, C. P.; Parent, J. L.; Turnbull, M. M. *Inorg. Chim. Acta* **2003**, *342*, 193.

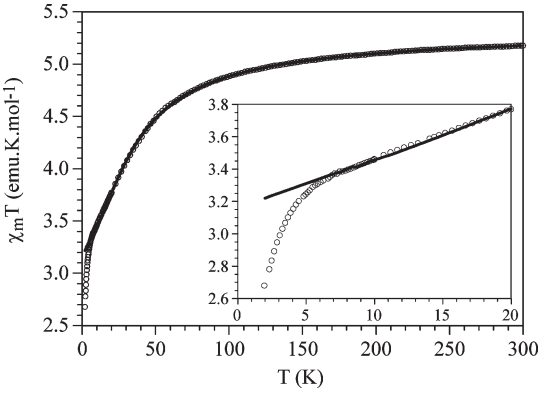

Figure 8. Thermal variation of the $\chi_m T$ product for compound **3**. Inset shows the low-temperature region. Solid line represents the best fit to the model (see text).

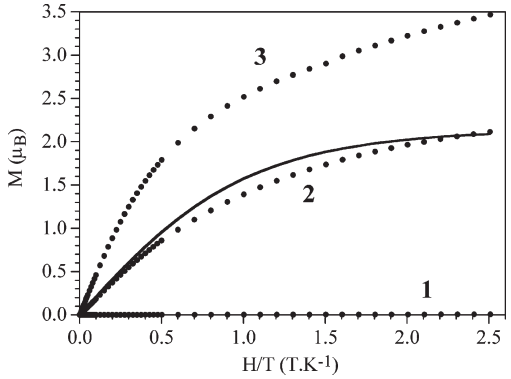

Figure 9. Isothermal magnetizations of compounds **1**, **2**, and **3** at 2 K. Solid line is the Brillouin function for an $S = 1$ spin state with $g = 2.149$ (see text).

pound **2** shows a magnetization plot typical of a paramagnetic $S = 1$ ground spin state, with a saturation value near 2 μ_B, although the experimental points are slightly below the expected values for an $S = 1$ ground spin state with the g value found in the fit of the magnetic data (solid line in Figure 9). This result confirms the $S = 1$ ground spin state resulting from the antiferromagnetic coupling in this compound as well as the existence of a zero field splitting in this $S = 1$ ground state (see above). Finally, compound **3** presents a magnetization plot well above that of compound **2** (Figure 9). Since the dinuclear complex in this compound does not present any contribution to the magnetization (as that of compound **1**), the magnetization of compound **3** is only due to the trinuclear complex. Therefore, the higher values observed in compound **3** indicate that its Ni_3 unit presents a ferromagnetic coupling, in agreement with the result obtained in the fit of the magnetic data. Although this ferromagnetic coupling leads to an $S = 3$ ground spin state for the trinuclear coupling, the magnetization data are well below the expected values for an $S = 3$ spin state (the saturation value should be $gS \approx 6\ \mu_B$). This fact can be attributed to the presence of a zero field splitting in the $S = 3$ ground state or to the very low value of the ferromagnetic coupling (less than 1 K) resulting in no saturation even at 5 T.

As expected, the dinuclear Ni(II) complexes present in compounds **1** and **3** are very similar from the structural and magnetic points of view, as demonstrated by the very similar antiferromagnetic couplings found in both compounds ($2J = -36.18(7)$ and $-29.5(1)$ K in **1** and **3**, respectively). In fact, the small differences in the coupling constant can be easily explained by the small differences in the geometrical parameters of the bridging Ni−O bonds (Table 2). Thus, although the average Ni−O bridging bond distances are very similar in both dinuclear complexes (2.063 and 2.062 Å in **1** and **3**, respectively), the Ni−O−Ni angles are slightly bigger in compound **1** (100.59° vs 99.39°). This difference agrees with the higher $2J$ value found in compound **1** (a higher angle gives rise to a higher antiferromagnetic coupling) since the magnetic coupling for doubly oxo-bridged Ni(II) complexes is expected to become more antiferromagnetic as the angle deviates from 90°.[23] A search in the CCDC database shows 12 similar Ni dimers with a N_2O_2 coordination environment around each Ni atom and a double oxo bridge.[24] Unfortunately, only one of these 12 Ni dimers reported to date has been magnetically characterized.[24] This compound presents a weak ferromagnetic coupling ($J = 3.04\ cm^{-1}$) that can be attributed to the smaller Ni−O−Ni bond angles (96.3° and 96.9°), compared with those of complexes **1** and **3A** (100.59° and 99.39°, respectively). Interestingly, in these 12 similar Ni dimers, there is always an additional bridge connecting the Ni atoms (usually one or two carboxylate bridges), and therefore, the Ni(II) dimers **1** and **3A** represent the first complexes of this type presenting exclusively a double oxo bridge.

Table 5. Bond Distances and Angles within the Bridges in the Dinuclear and Trinuclear Complexes of Compounds **1**, **2**, and **3**

compound	complex	$2J$ (K)	Ni−O (Å)	Ni−O (Å)	Ni−O−Ni (deg)
1	Ni_2	−36.18(7)	2.018(3)	2.109(2)	100.59(10)
2	Ni_3	−8.7(2)	2.065(2)	2.037(2)	96.49(8)
			2.085(2)	2.125(2)	99.90(9)
3	Ni_2	−29.5(1)	2.025(3)	2.099(3)	99.39(11)
	Ni_3	0.23(1)	2.019(3)	2.048(2)	91.87(10)
			2.137(2)	2.123(3)	97.63(11)

A different situation is found when comparing the magnetic coupling in the trinuclear complexes. Thus, although from the structural point of view both trinuclear clusters are similar, from the magnetic point of view they are quite different since the complex in compound **2** shows a weak antiferromagnetic coupling ($2J = -8.7$ K); whereas that in **3** shows a very weak, although ferromagnetic, coupling ($2J = 0.23$ K). Although this result is something unexpected, it can be explained from the structural differences found in complexes **2** and **3B**. Thus, if we compare both structures, we find that the average bridging Ni−O bond distances are very similar in both bridges and in both complexes (2.075 and 2.081 Å

(23) (a) Bertrand, J. A.; Ginsberg, A. P.; Kaplan, R. I.; Kirkwood, C. E.; Martin, R. L.; Sherwood, R. C. *Inorg. Chem.* **1971**, *10*, 240. (b) Juan, J. M. C.; Coronado, E.; Mascarós, J. R. G.; Gómez-García, C. J. *Inorg. Chem.* **1999**, *38*, 55.

(24) (a) Adams, H.; Clunas, S.; Fenton, D. E.; Spey, S. E. *J. Chem. Soc., Dalton Trans.* **2002**, 441. (b) Adams, H.; Fenton, D. E.; McHugh, P. E. *Inorg. Chem. Commun.* **2004**, *7*, 140. (c) Byun, J. C.; Lee, W. H.; Han, C. H. *Inorg. Chem. Cummun.* **2006**, *9*, 563. (d) Paital, A. R.; Mikuriya, M.; Ray, D. *Eur. J. Inorg. Chem.* **2007**, 5360.

in **2** and 2.078 and 2.085 Å in **3B**, Table 5). A second possible reason for the different magnetic behavior observed in the trimers could be the existence of significant differences in the syn−syn carboxylate bridges connecting the central Ni(II) ion with the terminal ones. Nevertheless, a close inspection of the structural parameters of both syn−syn carboxylate bridges shows no significant differences in the bond distances nor in the bond angles. It is clear, then, that the factor playing the most important role in determining the sign and magnitude of the magnetic coupling must be again the Ni−O−Ni bond angles. Thus, the Ni−O−Ni bond angles in compound **2** (99.89(9)° and 96.49(9)°, with an average value of 98.19°) are significantly larger than those of **3B** (97.63(11)° and 91.87(10)°, with an average value of 94.75°), in agreement with the weak antiferromagnetic and ferromagnetic couplings found in these complexes, respectively. A close inspection of the Ni_3 clusters in both compounds reveals that the smallest Ni−O−Ni angle observed in complex **3B** (Ni−O31−Ni = 91.87(10)°) is due to the fact that the bridging O31 atom belongs to a carboxylate chelating group, whereas in compound **2**, the equivalent bridging oxygen atom (O31) belongs to a monodentate carboxylate group, the other oxygen atom beinga water molecule (O100) (Figure 5).

It is also interesting to note that a search in the CCDC database shows up to 30 Ni trimers with a similar structure to those of complexes **2** and **3B** (a double oxo bridge plus a carboxylate bridge connecting the central Ni atoms with both external ones). Only 5 out of these 30 compounds have been magnetically characterized, and interestingly, they all show weak magnetic couplings (two of them are ferro- and the other three are antiferromagnetic) with J values in the range -3.4 to $+1.10$ cm^{-1}.[16,25]

(25) (a) Blake, A. J.; Brechin, E. K.; Codron, A.; Gould, R. O.; Grant, C. M.; Parsons, S.; Rawson, J. M.; Winpenny, R. E. P. *Chem. Commun.* **1995**, 1983. (b) Elmali, A.; Elerman, Y.; Svoboda, I.; Fuess, H.; Griesar, K.; Haase, W. *Z. Naturforsch., B: Chem. Sci.* **1996**, *51*, 665. (c) Kavlakoglu, E.; Elmali, A.; Elerman, Y.; Werner, R.; Svoboda, I.; Fuess, H. *Z. Naturforsch., B: Chem. Sci.* **2001**, *56*, 43. (d) Sharma, A. K.; Lloret, F.; Mukherjee, R. *Inorg. Chem.* **2007**, *46*, 5128.

The differences in sign and magnitude of the magnetic couplings observed in these five very closely related Ni(II) trimers demonstrate that very tiny structural changes may change the sign of the magnetic coupling in these Ni(II) trimers, as observed in complexes **2** and **3B**.

Conclusion

In conclusion, we have succeeded in preparing the very first example of isolated and cocrystallized Ni_2 and Ni_3 complexes after overcoming a series of synthetic challenges. The versatile coordination modes of the acetate ion allow the formation of dinuclear and trinuclear complexes by varying the stoichiometric ratio of the metal salt and the ligand. The similar crystal habits and the solubility of the dinuclear and trinuclear compounds in methanol seem to be responsible for the isolation of the cocrystal. Furthermore, the Ni_3 complex present in the cocrystal **3** represents also the first example of a trinuclear Ni(II) complex with an acetate group acting in the tridentate bridging mode $1\kappa^2OO':2\kappa O$. The structural and magnetic characterization of the cocrystal (**3**) and the pure forms (**1** and **2**) show that the Ni(II) dimers present in compounds **1** and **3** are structurally and magnetically almost identical with a moderate antiferromagnetic intradimer coupling. The Ni(II) trimers present in compounds **2** and **3** are structurally similar and present weak magnetic couplings (antiferromangnetic in compound **2** and ferromagnetic in compound **3**) that can be correlated with the slight structural differences observed in both complexes.

Acknowledgment. We thank CSIR, Government of India [Junior Research Fellowship to P.M., sanction no. 09/028 (0663)/2006-EMR-I] and EPSRC and the University of Reading for funds for the X-Calibur system. We also thank the European Union for financial support (MAGMANet network of excellence) and the Spanish Ministerio de Educación y Ciencia (Projects MAT2007-61584 and Consolider-Ingenio 2010 CSD 2007-00010 in Molecular Nanoscience).

Supporting Information Available: Crystallographic data in CIF format for the structures reported. This material is available free of charge via the Internet at http://pubs.acs.org.